FREE VIBRATIONS OF PLANAR SERIAL FRAME STRUCTURES IN THE CASE OF AXIALLY FUNCTIONALLY GRADED MATERIALS

Aleksandar Obradović, Slaviša Šalinić, and Aleksandar Tomović

Dedicated to the memory of Professor Veljko Vujičić

Abstract. This paper considers the problem of modal analysis and finding the closed-form solution to free vibrations of planar serial frame structures composed of Euler–Bernoulli beams of variable cross-sectional geometric characteristics in the case of axially functionally graded materials. Each of these beams is performing coupled axial and bending vibrations, where coupling occurs due to the boundary conditions at their joints. The numerical procedure for solving the system of partial differential equations, after the separation of variables, is reduced to solving the two-point boundary value problem of ordinary linear differential equations with nonlinear coefficients and linear boundary conditions. In this case, it is possible to transfer the boundary conditions and reduce the problem to the Cauchy initial value problem. Also, it is possible to analyze the influence of different parameters on the structure dynamic behavior. The method is applicable in the case of different boundary conditions at the right and left ends of such structures, as illustrated by an appropriate numerical example.

1. Introduction

Various engineering structures can be modeled as planar serial frame structures which consist of a finite number of rigidly connected Euler–Bernoulli beams, with different boundary conditions at the beginning and end of the beam. Due to the boundary conditions at the beam joints, coupling occurs between axial and bending vibrations although their differential equations are not coupled. In studying free vibrations of such structures it is certainly of interest to provide an applicable procedure that would be used for determining the natural frequencies, mode shapes, as well as the response of such systems to initial disturbances.

Paper [1] considers homogeneous beams of constant cross-sections within the framework of planar serial frame structures, so that the authors were able to find analytical solutions for appropriate partial differential equations of axial and bending vibrations and analytical form of the frequency equation, which is relatively easy to solve numerically. A more complex problem is discussed in [2], where elastic joints are introduced at the joints of homogeneous beams of the constant cross-section, while the solutions for equations are compared to the FEM analysis and experimental data. Paper [3] analyzes the portal frame structure, where mass discretization was carried out and a model with a finite number of DOFs was created instead of solving partial differential equations, and the results for such a model were verified by FEM. Coupled partial differential equations are also analytically solved in [4] in the case of planar multi-story frame structures. The authors of this paper managed to extend the analytical procedures presented in their papers [5,6] to solving the vibration problem of embedded rigid bodies to both the beams themselves and the ends of the structure. The procedure for obtaining analytical solutions for the governing equations of all sections of the structure depending on time is presented. In particular, the case of equality of all adjacent natural frequencies is analyzed.

When a cross-section along the beam axis changes, in a general case, there are no closed-form solutions for the system of differential equations, so they have to be solved numerically, as will be done in this paper, or a model with a relatively large number of DOFs has to be created by mass discretization. This conclusion also applies to the case of nonhomogeneous, axially functionally graded materials in which the material density and Young's modulus of elasticity change along the beam axis.

Crossing and veering phenomena can often occur in planar frame structures [7–10]. A change in the parameters of frame structures (such as the length of beams, angles between beams etc.) can lead to the intersect of the curves that show changes in values of natural frequencies of a frame structure due to the change in the observed structural parameter (the so-called crossing phenomena). Also, it may happen that the curves closely converge mutually in the close vicinity of the values of one structural parameter (the so-called veering phenomena). In this paper, we examine the possibility of crossing and veering phenomena in the frame structures here analyzed.

This paper is a continuation of the authors' research studies reported in paper [11] and doctoral dissertation [12], where they considered, among other things, individual Euler–Bernoulli beams of axially functionally graded materials, which are of variable cross-sectional characteristics and have complex boundary conditions at their ends due to fixed bodies or elastic elements. In [11] axial and bending vibrations were solved separately, because there was no coupling between them, whereas in [12] such coupling was analyzed including determination of the closed-form solution. The mentioned procedure related to individual beams is extended in this paper to planar serial frame structures. This extension is based on the use of the Symbolic-Numeric Method of Initial Parameters (SNMIP) proposed in [11]. The advantage of the SNMIP in computing natural frequencies over the often used dynamic stiffness matrix method [13–15] is observed through the fact that the

SNMIP is not based on the use of frequency equations with transcendental functions. This presents significant numerical simplification because the computation of natural frequencies from frequency equations with transcendental functions often requires the application of special numerical procedures such as the well-known Wittrick–Williams algorithm.

In Chapter 2 a coupled system of appropriate partial differential equations is derived with contour and initial conditions, and a well-known variable separation procedure and reduction to ordinary differential equations is conducted. Their modal analysis is performed in Chapter 3, which also enables the analysis of the influence of each parameter of the system on circular natural frequencies and mode shapes. Chapter 4 is dedicated to deriving the orthogonality conditions of mode shapes and determining the closed-form solution. The numerical example in Chapter 5 is used to illustrate the mentioned procedure in the case of different boundary conditions.

2. Problem statement

The paper considers planar serial frame structures, presented in Fig. 1, which consist of n Euler-Bernoulli beams of the known lengths L_i and angles α_i between them.
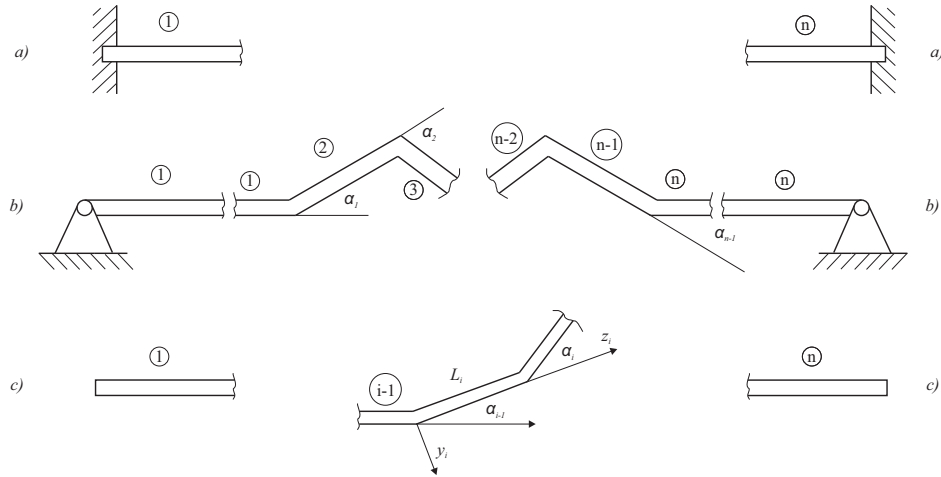

FIGURE 1. Planar serial frame structures with different boundary conditions: a) clamped; b) pinned; c) free

Differential equations of each of the Euler–Bernoulli beams, which are simultaneously oscillating in the axial and bending directions, are of the following form [16, 17]:

$$(2.1) \qquad \frac{\partial}{\partial z_i}[F_{T_i}(z_i, t)] - \rho_i(z_i)A_i(z_i)\frac{\partial^2 w_i(z_i, t)}{\partial t^2} = 0,$$

$$\frac{\partial}{\partial z_i}[F_{A_i}(z_i, t)] - \rho_i(z_i)A_i(z_i)\frac{\partial^2 u_i(z_i, t)}{\partial t^2} = 0, \quad i = 1, \ldots, n,$$

where $u_i(z_i, t)$ and $w_i(z_i, t)$ are axial and transverse displacements, the material density $\rho_i(z_i)$ in axially functionally graded materials is variable along the axis z_i the cross-sectional area $A_i(z_i)$ is also variable, and $F_{A_i}(z_i, t)$ and $F_{T_i}(z_i, t)$ represent axial and transverse forces:

$$F_{A_i}(z_i, t) = E_i(z_i)A_i(z_i)\frac{\partial u_i(z_i, t)}{\partial z_i},$$

$$F_{T_i}(z_i, t) = \frac{\partial M_{F_i}(z_i, t)}{\partial z_i},$$

where $E_i(z_i)$ is variable Young's modulus of elasticity, with the bending moment given by the expression

$$M_{F_i}(z_i, t) = -E_i(z_i)I_{x_i}(z_i)\frac{\partial^2 w_i(z_i, t)}{\partial z_i^2},$$

where $I_{x_i}(z_i)$ represents the cross-sectional area moment of inertia. Note that differential equations can also be derived from a corresponding integro-differential equation, as has already been done in the book by Professor Vujičić [18].

At the beam joints the following boundary conditions exist:

(2.2)
$$u_{i+1}(0, t) = u_i(L_i, t)\cos\alpha_i - w_i(L_i, t)\sin\alpha_i$$
$$w_{i+1}(0, t) = u_i(L_i, t)\sin\alpha_i + w_i(L_i, t)\cos\alpha_i$$
$$\frac{\partial w_{i+1}(0, t)}{\partial z_{i+1}} = \frac{\partial w_i(L_i, t)}{\partial z_i}$$
$$F_{A_{i+1}}(0, t) = F_{A_i}(L_i, t)\cos\alpha_i - F_{T_i}(L_i, t)\sin\alpha_i$$
$$F_{T_{i+1}}(0, t) = F_{A_i}(L_i, t)\sin\alpha_i + F_{T_i}(L_i, t)\cos\alpha_i$$
$$M_{F_{i+1}}(0, t) = M_{F_i}(L_i, t)$$

At the left end of this complex structure, depending on whether the first beam is: a) clamped, b) pinned, or c) free, the boundary conditions are of the following form:

a) $\qquad u_1(0, t) = 0, \quad w_1(0, t) = 0, \quad \dfrac{\partial w_1(0, t)}{\partial z_1} = 0$

b) $\qquad u_1(0, t) = 0, \quad w_1(0, t) = 0, \quad M_{F_1}(0, t) = 0$

c) $\qquad F_{A_1}(0, t) = 0, \quad F_{T_1}(0, t) = 0, \quad M_{F_1}(0, t) = 0.$

The boundary conditions at the right end of the structure, which will be the subject of consideration in the present paper, are of the form:

a) $\qquad u_n(L_n, t) = 0, \quad w_n(L_n, t) = 0, \quad \dfrac{\partial w_n(L_n, t)}{\partial z_n} = 0$

b) $\qquad u_n(L_n, t) = 0, \quad w_n(L_n, t) = 0, \quad M_{F_n}(L_n, t) = 0$

c) $\qquad F_{A_n}(L_n, t) = 0, \quad F_{T_n}(L_n, t) = 0, \quad M_{F_n}(L_n, t) = 0.$

Free vibrations of such a structure are considered under the following initial conditions:

$$u_i(z_i, 0) = f_{u_i}(z_i), \quad \frac{\partial u_i(z_i, 0)}{\partial t} = h_{u_i}(z_i),$$

$$w_i(z_i, 0) = f_{w_i}(z_i), \quad \frac{\partial w_i(z_i, 0)}{\partial t} = h_{w_i}(z_i), \qquad i = 1, \dots, n$$

The linear differential equations (2.1) are solved by the variable separation method [9, 10]:

$$w_i(z_i, t) = W_i(z_i)T(t), \quad w_{D_i}(z_i, t) = \frac{\partial W_i(z_i, t)}{\partial z_i} = \frac{\partial W_i(z_i)}{\partial z_i}T(t) = W_{d_i}(z_i)T(t),$$

$$u_i(z_i, t) = U_i(z_i)T(t), \quad F_{A_i}(z_i, t) = F_{a_i}(z_i)T(t),$$

$$F_{T_i}(z_i, t) = F_{t_i}(z_i)T(t), \quad M_{F_i}(z_i, t) = M_{f_i}(z_i)T(t),$$

where the coupling between axial and bending vibrations under boundary conditions (2.2) leads to the fact that the function of time $T(t)$ is the same for both types of vibrations in all beams, for which it holds

$$\frac{\partial^2 T(t)}{\partial t^2} = -\omega^2 T(t),$$

where ω is a circular natural frequency.

This way, a corresponding system of six linear ordinary differential equations with variable coefficients can be written for each beam:

$$\frac{\partial U_i(z_i)}{\partial z_i} = \frac{F_{a_i}(z_i)}{E_i(z_i)A_i(z_i)}, \quad \frac{\partial W_i(z_i)}{\partial z_i} = W_{d_i}(z_i), \quad \frac{\partial W_{d_i}(z_i)}{\partial z_i} = \frac{-M_{f_i}(z_i)}{E_i(z_i)I_{x_i}(z_i)},$$

(2.3) $\quad \dfrac{\partial F_{a_i}(z_i)}{\partial z_i} = -\omega^2 \rho_i(z_i)A_i(z_i)U_i(z_i), \quad \dfrac{\partial F_{t_i}(z_i)}{\partial z_i} = -\omega^2 \rho_i(z_i)A_i(z_i)W_i(z_i),$

$$\frac{\partial M_{f_i}(z_i)}{\partial z_i} = F_{t_i}(z_i),$$

while the boundary conditions at beam joints are:

$$U_{i+1}(0) = U_i(L_i)\cos\alpha_i - W_i(L_i)\sin\alpha_i,$$

$$W_{i+1}(0) = U_i(L_i)\sin\alpha_i + W_i(L_i)\cos\alpha_i$$

$$W_{d_{i+1}}(0) = W_{d_i}(L_i)$$

(2.4)

$$F_{a_{i+1}}(0) = F_{a_i}(L_i)\cos\alpha_i - F_{t_i}(L_i)\sin\alpha_i$$

$$F_{t_{i+1}}(0) = F_{a_i}(L_i)\sin\alpha_i + F_{t_i}(L_i)\cos\alpha_i$$

$$M_{f_{i+1}}(0) = M_{f_i}(L_i),$$

at the left end:

$$\begin{array}{llll} & \text{a)} & U_1(0) = 0, \quad W_1(0) = 0, & W_{d_1}(0) = 0 \\ (2.5) & \text{b)} & U_1(0) = 0, \quad W_1(0) = 0, & M_{f_1}(0) = 0 \\ & \text{c)} & F_{a_1}(0) = 0, \quad F_{t_1}(0) = 0, & M_{f_1}(0) = 0 \end{array}$$

and at the right end:

$$
\begin{array}{lllll}
& \text{a)} & U_n(L_n) = 0, & W_n(L_n) = 0, & W_{d_n}(L_n) = 0 \\
(2.6) & \text{b)} & U_n(L_n) = 0, & W_n(L_n) = 0, & M_{f_n}(L_n) = 0 \\
& \text{c)} & F_{a_n}(L_n) = 0, & F_{t_n}(L_n) = 0, & M_{f_n}(L_n) = 0,
\end{array}
$$

also linear. So, instead of numerically solving the system of $6n$ differential equations (2.3) with the same number of boundary conditions (2.4)–(2.6), this enables us to reduce the problem to numerical solving of the Cauchy problem [19]. Thereafter, in each concrete case the frequency equation would be simply generated and solved, and natural frequencies and mode shapes would be determined. That procedure is presented in Chapter 3 of the paper.

Here, note that in a general case this problem needs to be numerically solved but also solving the Cauchy problem, frequency equation, as well as calculating the mode shapes is a part of standard numerical procedures that can be found in various program packages. In this paper, our option was the package MATHEMATICA® [20].

3. Modal analysis of coupled axial and bending vibrations

Considering the linearity (2.3)–(2.6), the solution can be sought, depending on the value of the circular natural frequency ω, as a linear form of three different solutions for the system (2.3), (2.4):

$$
\boldsymbol{X}_i(z_i) = C_1 \boldsymbol{X}_i^1(z_i) + C_2 \boldsymbol{X}_i^2(z_i) + C_3 \boldsymbol{X}_i^3(z_i),
$$

where

$$
\boldsymbol{X}_i(z_i) = [U_i(z_i), W_i(z_i), W_{d_i}(z_i), F_{a_i}(z_i), F_{t_i}(z_i), M_{f_i}(z_i)]^T
$$
$$
\boldsymbol{X}_i^k(z_i) = [U_i^k(z_i), W_i^k(z_i), W_{d_i}^k(z_i), F_{a_i}^k(z_i), F_{t_i}^k(z_i), M_{f_i}^k(z_i)]^T, \quad k = 1, 2, 3.
$$

The solutions $\boldsymbol{X}_i^k(z_i)$ are obtained by successive numerical solving of the system (2.3) starting from the first beam, where the initial conditions $\boldsymbol{X}_1^k(0)$ must be selected to satisfy the conditions (2.5). This can be done for the cases considered herein, in the following manner:

$$
\begin{array}{lllll}
& \text{a)} & \boldsymbol{X}_1^1(0) = [0,0,0,1,0,0]^T, & \boldsymbol{X}_1^2(0) = [0,0,0,0,1,0]^T, & \boldsymbol{X}_1^3(0) = [0,0,0,0,0,1]^T \\
(3.1) & \text{b)} & \boldsymbol{X}_1^1(0) = [0,0,1,0,0,0]^T, & \boldsymbol{X}_1^2(0) = [0,0,0,1,0,0]^T, & \boldsymbol{X}_1^3(0) = [0,0,0,0,1,0]^T \\
& \text{c)} & \boldsymbol{X}_1^1(0) = [1,0,0,0,0,0]^T, & \boldsymbol{X}_1^2(0) = [0,1,0,0,0,0]^T, & \boldsymbol{X}_1^3(0) = [0,0,1,0,0,0]^T.
\end{array}
$$

For each of these solutions the boundary conditions (2.4) also hold, and they can be written in the form:

$$
(3.2) \qquad \boldsymbol{X}_{i+1}^k(0) = \boldsymbol{K}_i \boldsymbol{X}_i^k(L_i),
$$

where

$$
\boldsymbol{K}_i =
\begin{bmatrix}
\cos\alpha_i & -\sin\alpha_i & 0 & 0 & 0 & 0 \\
\sin\alpha_i & \cos\alpha_i) & 0 & 0 & 0 & 0 \\
0 & 0 & 1 & 0 & 0 & 0 \\
0 & 0 & 0 & \cos\alpha_i & -\sin\alpha_i & 0 \\
0 & 0 & 0 & -\sin\alpha_i & \cos\alpha_i & 0 \\
0 & 0 & 0 & 0 & 0 & 1
\end{bmatrix}
$$

This set of Cauchy problems, considering that the form of differential equations (2.3) for specified ω has a unique solution, can use the command NDSolve[...] in the package MATHEMATICA® [20]. If these solutions are sought for different values of ω, the command ParametricNDSolve[...,{ω }] is available. However, only solutions that satisfy boundary conditions at the right end of the structure (2.6) are of interest, which leads to a homogeneous system of linear equations

$$(3.3) \qquad \boldsymbol{D}(\omega)\boldsymbol{C} = \boldsymbol{0}, \quad \boldsymbol{D}(\omega) = \begin{bmatrix} d_{11}(\omega) & d_{12}(\omega) & d_{13}(\omega) \\ d_{21}(\omega) & d_{22}(\omega) & d_{23}(\omega) \\ d_{31}(\omega) & d_{32}(\omega) & d_{33}(\omega) \end{bmatrix}, \quad \boldsymbol{C} = \begin{bmatrix} C_1 \\ C_2 \\ C_3 \end{bmatrix},$$

where the matrix $\boldsymbol{D}(\omega)$ in different cases of boundary conditions at the right end is of the form:

$$\text{a)} \qquad \boldsymbol{D}(\omega) = \begin{bmatrix} U_n^1(L_n) & U_n^2(L_n) & U_n^3(L_n) \\ W_n^1(L_n) & W_n^2(L_n) & W_n^3(L_n) \\ W_{d_n}^1(L_n) & W_{d_n}^2(L_n) & W_{d_n}^3(L_n) \end{bmatrix}$$

$$\text{b)} \qquad \boldsymbol{D}(\omega) = \begin{bmatrix} U_n^1(L_n) & U_n^2(L_n) & U_n^3(L_n) \\ W_n^1(L_n) & W_n^2(L_n) & W_n^3(L_n) \\ M_{f_n}^1(L_n) & M_{f_n}^2(L_n) & M_{f_n}^3(L_n) \end{bmatrix}$$

$$\text{c)} \qquad \boldsymbol{D}(\omega) = \begin{bmatrix} F_{a_n}^1(L_n) & F_{a_n}^2(L_n) & F_{a_n}^3(L_n) \\ F_{t_n}^1(L_n) & F_{t_n}^2(L_n) & F_{t_n}^3(L_n) \\ M_{f_n}^1(L_n) & M_{f_n}^2(L_n) & M_{f_n}^3(L_n) \end{bmatrix}$$

The frequency equation now reads:

$$(3.4) \qquad\qquad F(\omega) = \det(\boldsymbol{D}(\omega)) = 0.$$

The function $F(\omega)$ can also be graphically represented in a simple way, and the finite number of its zeros ω_α, $\alpha = 1, \ldots, \infty$ can be numerically calculated as well. The values of circular natural frequencies are matched by the solutions $\boldsymbol{X}_{i\alpha}^k(z_i) = [U_{i\alpha}^k(z_i), W_{i\alpha}^k(z_i), W_{d_{i\alpha}}^k(z_i), F_{a_{i\alpha}}^k(z_i), F_{t_{i\alpha}}^k(z_i), M_{f_{i\alpha}}^k(z_i)]^T$. A general solution for the system (2.3) now becomes the sum of particular solutions

$$\boldsymbol{X}_i(z_i) = \sum_{\alpha=1}^{\infty} C_{1\alpha}\boldsymbol{X}_{i\alpha}^*(z_i)$$

where the functions of the mode shapes

$$\boldsymbol{X}_{i\alpha}^*(z_i) = [U_{i\alpha}^*(z_i), W_{i\alpha}^*(z_i), W_{d_{i\alpha}}^*(z_i), F_{a_{i\alpha}}^*(z_i), F_{t_{i\alpha}}^*(z_i), M_{f_{i\alpha}}^*(z_i)]^T$$
$$= \boldsymbol{X}_{i\alpha}^1(z_i) + \frac{C_{2\alpha}}{C_{1\alpha}}\boldsymbol{X}_{i\alpha}^2(z_i) + \frac{C_{3\alpha}}{C_{1\alpha}}\boldsymbol{X}_{i\alpha}^3(z_i)$$

are completely determined for each mode shape, because from the system (3.3) it follows

$$(3.5) \qquad\qquad \frac{C_{2\alpha}}{C_{1\alpha}} = \frac{d_{21}(\omega_\alpha)d_{13}(\omega_\alpha) - d_{11}(\omega_\alpha)d_{23}(\omega_\alpha)}{d_{12}(\omega_\alpha)d_{23}(\omega_\alpha) - d_{22}(\omega_\alpha)d_{13}(\omega_\alpha)},$$
$$\frac{C_{3\alpha}}{C_{1\alpha}} = \frac{d_{22}(\omega_\alpha)d_{11}(\omega_\alpha) - d_{12}(\omega_\alpha)d_{21}(\omega_\alpha)}{d_{12}(\omega_\alpha)d_{23}(\omega_\alpha) - d_{22}(\omega_\alpha)d_{13}(\omega_\alpha)}.$$

If it is of interest to analyze the influence of some parameter p on the dynamic behavior of this structure, primarily on the values of its natural frequencies, this procedure can be slightly modified and dependence of natural frequencies on that parameter can be obtained. In that case, all numerical solutions would be sought in the function of two parameters, ω and p, and the dependence sought would follow from the frequency equation (3.4), which would now be of the form

$$(3.6) \qquad F(\omega, p) = \det(\boldsymbol{D}(\omega, p)) = 0$$

4. Orthogonality conditions of mode shapes and the closed-form solution

Orthogonality conditions of the mode shapes can be found in the literature [16,17] for a single body and separately for axial and bending vibrations. For the needs of this paper, where coupling between axial and bending vibrations exists, as well as a larger number of beams, the orthogonality conditions are somewhat more complex. Here, we will describe the procedure which represents generalization for the case of homogeneous bodies of a constant cross-section, as reported in our paper [6].

Let $U_{i\alpha}(z_i)$ and $W_{i\alpha}(z_i)$ be the solutions corresponding to the circular natural frequency ω_α and let $U_{i\beta}(z_i)$ and $W_{i\beta}(z_i)$ correspond to the circular natural frequency ω_β. Then, from differential equations (2.3), written for the case of the mentioned natural frequencies, it follows

$$(\omega_\alpha^2 - \omega_\beta^2) \int_0^{L_i} \rho_i(z_i) A_i(z_i) U_{i\alpha}(z_i) U_{i\beta}(z_i) dz_i$$
$$= \int_0^{L_i} \Big(-\frac{\partial F_{a_{i\alpha}}(z_i)}{\partial z_i} U_{i\beta}(z_i) + \frac{\partial F_{a_{i\beta}}(z_i)}{\partial z_i} U_{i\alpha}(z_i) \Big) dz_i$$

$$(\omega_\alpha^2 - \omega_\beta^2) \int_0^{L_i} \rho_i(z_i) A_i(z_i) W_{i\alpha}(z_i) W_{i\beta}(z_i) dz_i$$
$$= \int_0^{L_i} \Big(-\frac{\partial F_{t_{i\alpha}}(z_i)}{\partial z_i} W_{i\beta}(z_i) + \frac{\partial F_{t_{i\beta}}(z_i)}{\partial z_i} U_{i\alpha}(z_i) \Big) dz_i$$

where it is noticeable that

$$-\frac{\partial F_{a_{i\alpha}}(z_i)}{\partial z_i} U_{i\beta}(z_i) + \frac{\partial F_{a_{i\beta}}(z_i)}{\partial z_i} U_{i\alpha}(z_i) = \frac{\partial(-F_{a_{i\alpha}}(z_i) U_{i\beta}(z_i) + F_{a_{i\beta}}(z_i) U_{i\alpha}(z_i))}{\partial z_i}$$

$$-\frac{\partial F_{t_{i\alpha}}(z_i)}{\partial z_i} W_{i\beta}(z_i) + \frac{\partial F_{t_{i\beta}}(z_i)}{\partial z_i} W_{i\alpha}(z_i)$$
$$= \frac{\partial(-F_{t_{i\alpha}}(z_i) W_{i\beta}(z_i) + M_{f_{i\alpha}}(z_i) W_{d_{i\beta}}(z_i) + F_{t_{i\beta}}(z_i) W_{i\alpha}(z_i) - M_{f_{i\beta}}(z_i) W_{d_{i\alpha}}(z_i))}{\partial z_i},$$

from which it follows

$$(4.1) \quad (\omega_\alpha^2 - \omega_\beta^2) \int_0^{L_i} \rho_i(z_i) A_i(z_i) (U_{i\alpha}(z_i) U_{i\beta}(z_i) + W_{i\alpha}(z_i) W_{i\beta}(z_i)) dz_i$$
$$= \big(-F_{a_{i\alpha}}(L_i) U_{i\beta}(L_i) + F_{a_{i\beta}}(L_i) U_{i\alpha}(L_i) - F_{t_{i\alpha}}(L_i) W_{i\beta}(L_i)$$

$$+ M_{f_{i\alpha}}(L_i)W_{d_{i\beta}}(L_i) + F_{t_{i\beta}}(L_i)W_{i\alpha}(L_i) - M_{f_{i\beta}}(L_i)W_{d_{i\alpha}}(L_i)\big)$$
$$- \big(- F_{a_{i\alpha}}(0)U_{i\beta}(0) + F_{a_{i\beta}}(0)U_{i\alpha}(0) - F_{t_{i\alpha}}(0)W_{i\beta}(0) + M_{f_{i\alpha}}(0)W_{d_{i\beta}}(0)$$
$$+ F_{t_{i\beta}}(0)W_{i\alpha}(0) - M_{f_{i\beta}}(0)W_{d_{i\alpha}}(0)\big).$$

If the conditions (2.4)–(2.6) are written for the cases corresponding to the mentioned natural frequencies and are inserted into (4.1), it is noticeable that

$$\sum_{i=1}^{n} \big(- F_{a_{i\alpha}}(L_i)U_{i\beta}(L_i) + F_{a_{i\beta}}(L_i)U_{i\alpha}(L_i) - F_{t_{i\alpha}}(L_i)W_{i\beta}(L_i)$$
$$+ M_{f_{i\alpha}}(L_i)W_{d_{i\beta}}(L_i) + F_{t_{i\beta}}(L_i)W_{i\alpha}(L_i) - M_{f_{i\beta}}(L_i)W_{d_{i\alpha}}(L_i)\big)$$
$$- \big(- F_{a_{i\alpha}}(0)U_{i\beta}(0) + F_{a_{i\beta}}(0)U_{i\alpha}(0) - F_{t_{i\alpha}}(0)W_{i\beta}(0) + M_{f_{i\alpha}}(0)W_{d_{i\beta}}(0)$$
$$+ F_{t_{i\beta}}(0)W_{i\alpha}(0) - M_{f_{i\beta}}(0)W_{d_{i\alpha}}(0)\big) = 0$$

so that the orthogonality conditions have the form

$$(4.2) \quad (\omega_\alpha^2 - \omega_\beta^2) \sum_{i=1}^{n} \int_0^{L_i} \rho_i(z_i)A_i(z_i)\big(U_{i\alpha}(z_i)U_{i\beta}(z_i) + W_{i\alpha}(z_i)W_{i\beta}(z_i)\big)dz_i = 0,$$

from which it follows

$$\sum_{i=1}^{n} \int_0^{L_i} \rho_i(z_i)A_i(z_i)\big(U_{i\alpha}(z_i)U_{i\beta}(z_i) + W_{i\alpha}(z_i)W_{i\beta}(z_i)\big)dz_i = 0, \quad \alpha \neq \beta.$$

Considering that

$$U_{i\alpha}(z_i) = C_{1\alpha}U_{i\alpha}^*(z_i), \quad W_{i\alpha}(z_i) = C_{1\alpha}W_{i\alpha}^*(z_i),$$
$$U_{i\beta}(z_i) = C_{1\beta}U_{i\beta}^*(z_i), \quad W_{i\beta}(z_i) = C_{1\beta}W_{i\beta}^*(z_i),$$

the conditions (4.2) also apply to the functions of the mode shapes considered in Chapter 3:

$$(4.3) \quad \sum_{i=1}^{n} \int_0^{L_i} \rho_i(z_i)A_i(z_i)\big(U_{i\alpha}^*(z_i)U_{i\beta}^*(z_i) + W_{i\alpha}^*(z_i)W_{i\beta}^*(z_i)\big)dz_i = 0, \quad \alpha \neq \beta.$$

These conditions are necessary to obtain the closed-form solutions. The function of time that corresponds to the circular natural frequency ω_α is of the form:

$$T_\alpha(t) = A_\alpha \cos(\omega_\alpha t) + B_\alpha \sin(\omega_\alpha t),$$

so that the final solutions for axial and transverse displacements can be written as:

$$(4.4) \quad u_i(z_i, t) = \sum_{\alpha=1}^{\infty} U_{i\alpha}^*(z_i)\big(A_\alpha^* \cos(\omega_\alpha t) + B_\alpha^* \sin(\omega_\alpha t)\big),$$

$$w_i(z_i, t) = \sum_{\alpha=1}^{\infty} W_{i\alpha}^*(z_i)\big(A_\alpha^* \cos(\omega_\alpha t) + B_\alpha^* \sin(\omega_\alpha t)\big),$$

where $A_\alpha^* = C_{1\alpha}A_\alpha$, $B_\alpha^* = C_{1\alpha}B_\alpha$.

By using the orthogonality conditions (4.3), we also obtain the solutions for constants in the functions $T_\alpha(t)$

$$(4.5) \qquad A_\alpha^* = \frac{\sum_{i=1}^n \int_0^{L_i} \rho_i(z_i) A_i(z_i)(U_{i\alpha}^*(z_i) f_{u_i}(z_i) + W_{i\alpha}^*(z_i) f_{w_i}(z_i)) dz_i}{\sum_{i=1}^n \int_0^{L_i} \rho_i(z_i) A_i(z_i)(U_{i\alpha}^*(z_i)^2 + W_{i\alpha}^*(z_i)^2) dz_i}$$

$$B_\alpha^* = \frac{1}{\omega_\alpha} \frac{\sum_{i=1}^n \int_0^{L_i} \rho_i(z_i) A_i(z_i)(U_{i\alpha}^*(z_i) h_{u_i}(z_i) + W_{i\alpha}^*(z_i) h_{w_i}(z_i)) dz_i}{\sum_{i=1}^n \int_0^{L_i} \rho_i(z_i) A_i(z_i)(U_{i\alpha}^*(z_i)^2 + W_{i\alpha}^*(z_i)^2) dz_i},$$

which completes the procedure of finding the closed-form solutions. It should be noted that the integrals in the expressions (4.5), as well as all other solutions in this paper, are possible to solve only numerically, because the authors' intention is that the procedure should apply in a general case to arbitrary change of cross-section, as well as to axially functionally graded materials.

5. Numerical example

The presented procedure will be illustrated by an example of the planar serial frame structures which consist of $n = 3$ equal beams of variable circular cross-section, diameter D_i, made of axially functionally graded material, where:

$$L_i = L, \quad D_i(z_i) = D_0\Big(1 - 0.1\frac{z_i}{L}\Big), \quad E_i(z_i) = E_0\Big(1 - 0.1\sin\frac{\pi z_i}{L}\Big),$$

$$\rho_i(z_i) = \rho_0\Big(1 - 0.1\sin\frac{\pi z_i}{L}\Big), \qquad i = 1, 2, 3,$$

with numerical values of the parameters:

$$L = 1\,\mathrm{m}, \quad D_0 = 0.05\,\mathrm{m}, \quad E_0 = 2.068 \cdot 10^{11}\,\mathrm{N/m}^2, \quad \rho_0 = 7850\,\mathrm{kg/m}^3.$$

We will also take that the angles between adjacent beams are equal, $\alpha_1 = \alpha_2 = p$, and we will analyze the dynamic behavior in terms of that parameter, angle p. The analysis will involve three cases of connecting the structure at the right and left end: clamped-clamped, clamped-pinned and clamped-free, as presented in Figure 2 (a, b, and c), respectively.
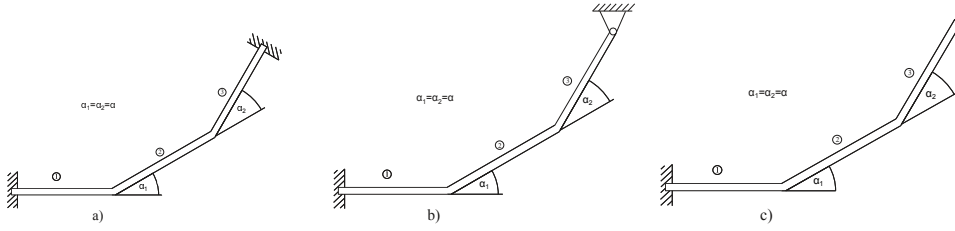

FIGURE 2. Initial positions of frame structures with various boundary conditions: a) clamped-clamped; b) clamped-pinned; c) clamped-free

Dependencies of the first four natural frequencies on the parameter p, in the considered cases, are displayed consecutively in Figures 3, 4 and 5 based on implicit dependence $F(\omega, p) = 0$.
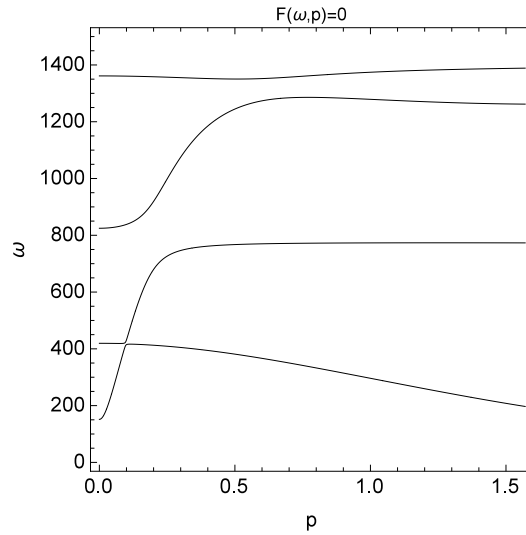

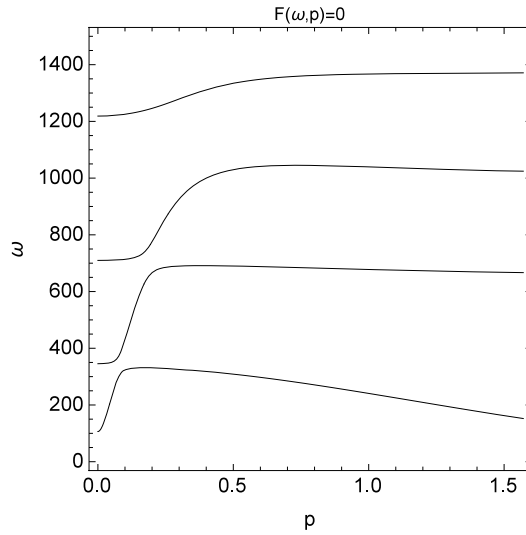FIGURE 3. Representation of the function $F(\omega, p) = 0$ in the case of clamped-clamped boundary conditions

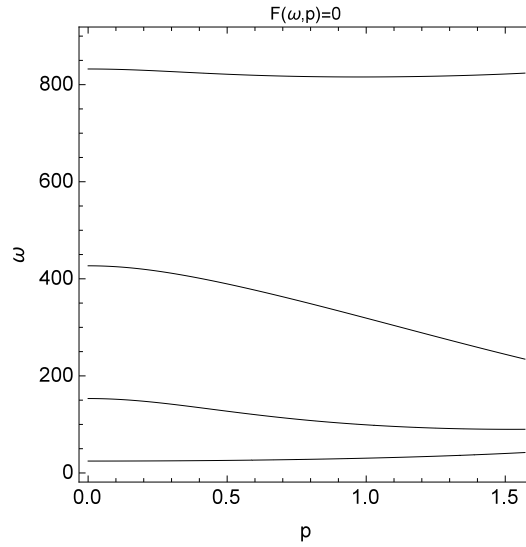FIGURE 4. Representation of the function $F(\omega, p) = 0$ in the case of clamped-pinned boundary conditions

FIGURE 5. Representation of the function $F(\omega, p) = 0$ in the case of clamped-free boundary conditions

All the presented graphs indicate clearly the influence of the angle p on each of the four first natural frequencies, as well as the difference between these diagrams depending on the mode of the structure support. It can also be clearly seen that the values of natural frequencies are the highest in the first considered case and the lowest in the third one.

A well-known veering phenomenon is noted in the first considered case [7–9], where two adjacent natural frequencies converge for specific parameter values. The initial position of the frame structure for the small values of the angle p is presented in Figure 6.
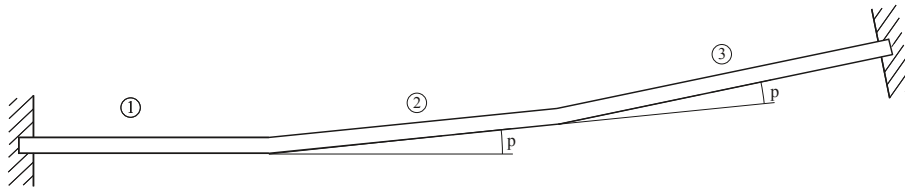

FIGURE 6. The initial position of the frame structure with clamped ends in the case of veering, $(p = 0.1)$

In this case, the basic and second natural frequency converge, as shown in Figure 7.

The procedure of determining circular natural frequencies and the functions of mode shapes will be conducted in the clamped-clamped case for $p = \frac{\pi}{4}$.
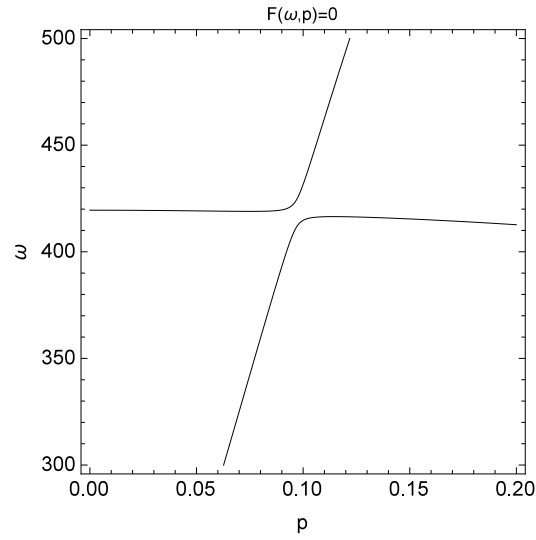
F(ω,p)=0

FIGURE 7. Veering phenomenon in the case of the frame structure with clamped ends
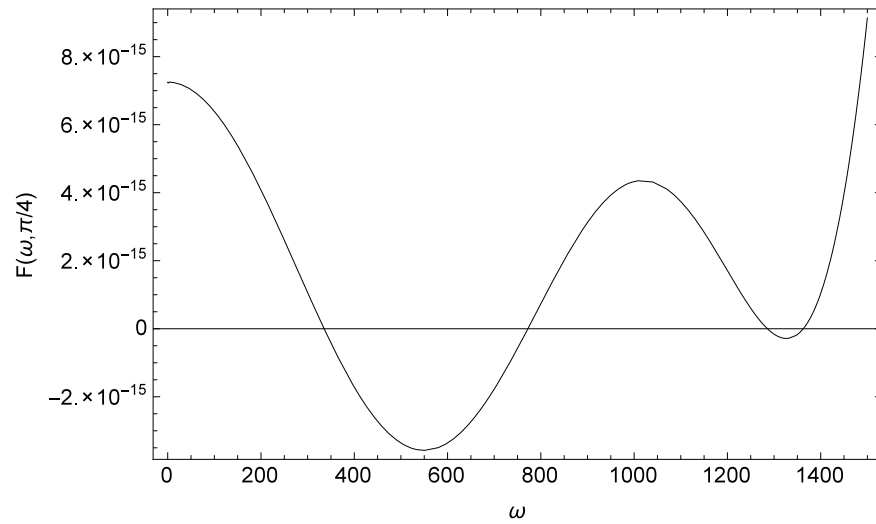

FIGURE 8. Graph of the function $F(\omega)$ in the clamped-clamped case for $p = \pi/4$

The graph of the function $F(\omega)$ is shown in Figure 8 and its first four zeros are simply numerically calculated and are given in Table 1.

Thereafter, for each of the natural frequencies the Cauchy problems with differential equations are solved (2.3), starting from the first body with initial conditions

TABLE 1. First four circular natural frequencies in the clamped-clamped case, $p = \pi/4$

ω_1 [Hz]	ω_2 [Hz]	ω_3 [Hz]	ω_4 [Hz]
335.356	772.214	1285.829	1362.564

(3.1)a and conditions (3.2) at the body joints. When obtaining the functions of mode shapes $\boldsymbol{X}_{i\alpha}^*(z_i)$ it is necessary to calculate previously the coefficients in the expressions (3.5). For illustration purposes, Figure 9 presents mode shapes for the first body, which correspond to transverse displacements in the first four mode shapes ($W_{1\alpha}^*(z_1)$, $\alpha = 1, \ldots, 4$) respectively.
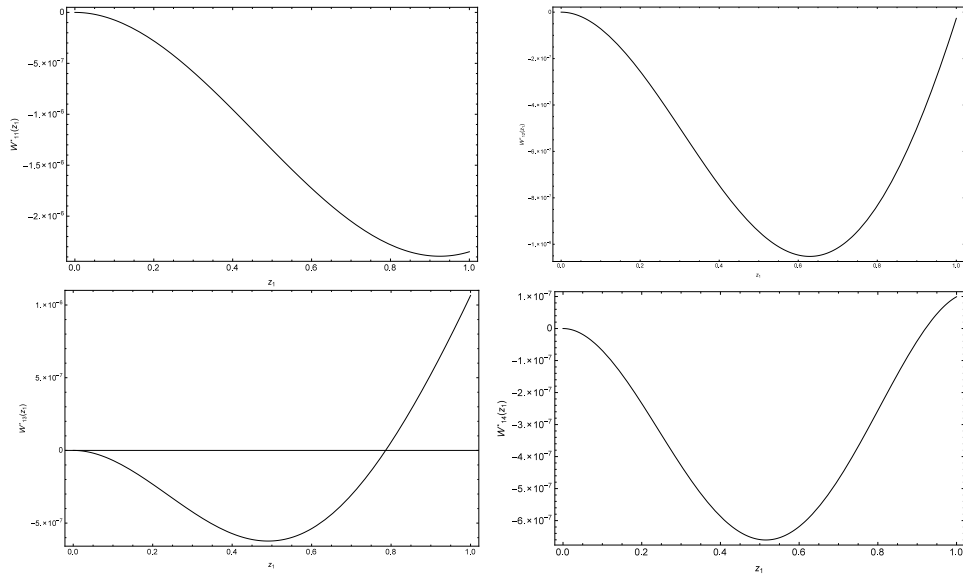
FIGURE 9. Graphs of the functions $W_{1\alpha}^*(z_1)$, $\alpha = 1, \ldots, 4$ in the clamped-clamped case for $p = \pi/4$

Note here that this procedure can be efficiently applied in testing possible equalization of adjacent natural frequencies for specific values of the parameter p, a well-known crossing phenomenon in the literature [7, 10]. It is then that the two adjacent lines in diagrams $F(\omega, p) = 0$ are intersecting, unlike the veering phenomenon, where they are converging. If in the clamped-clamped case we consider the homogeneous material ($E_i(z_i) = E_0$ $\rho_i(z_i) = \rho_0$), where each rod diameter is constant ($D_i(z_i) = D_0$), the structure is completely symmetrical. Dependence of natural frequencies on the angle p is shown in Figure 10.

Equalization of the first two natural frequencies $\omega_1 = \omega_2 = 437.866$ Hz is noted for the value $p^* = 0.101074$ rad, as shown in Figure 11.
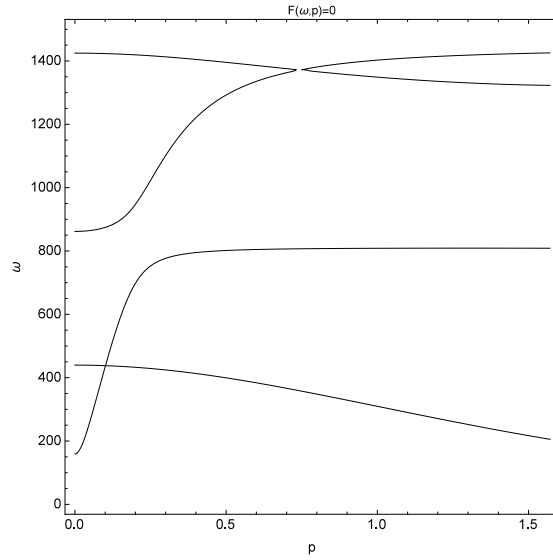
FIGURE 10. Representation of the function $F(\omega, p) = 0$ in the case of the clamped-clamped symmetrical structure
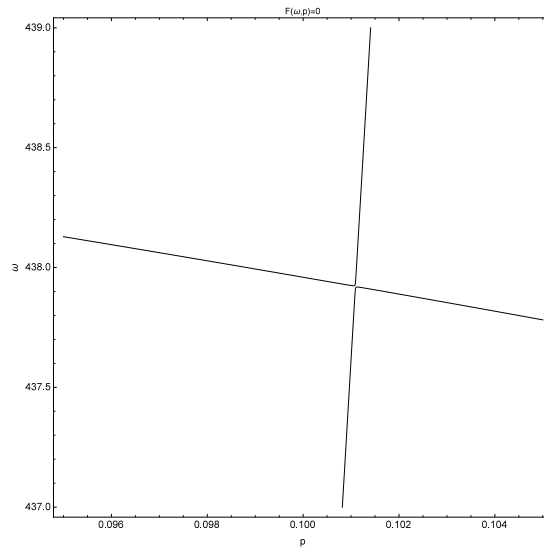
FIGURE 11. Crossing phenomenon in the case of the clamped-clamped symmetrical structure

By changing the parameter p in the neighborhood of p^* the first and second mode shape immediately exchange their places. However, the orthogonality conditions of these mode shapes do not hold for $p = p^*(\omega_1 = \omega_2)$, and therefore for the final solutions either (4.4). The corresponding expressions in that case of equal-

ized adjacent natural frequencies can be found in the authors' paper [6] for the case of homogeneous beams of a constant cross-section, and can be relatively easily generalized to the problem treated in this paper.

The method, developed in [6], can be applied in forming the transcendental frequency equation (3.6) that can be solved numerically in order for values of circular natural frequencies for the given values of the parameter p to be obtained. It should be noted that there are analytical solutions for the system (2.3) with boundary conditions (2.4)–(2.6) for homogeneous beams with a constant cross-sectional area. In Table 2 the comparative values of the first two natural frequencies are presented. The numerical values are computed using the method presented in this paper, FEM analysis (Ansys, element type BEAM 189, Number of total elements 304) and numerical solution for the exact frequency equation [6].

TABLE 2. The first two circular natural frequencies in the vicinity of $p = p^*$

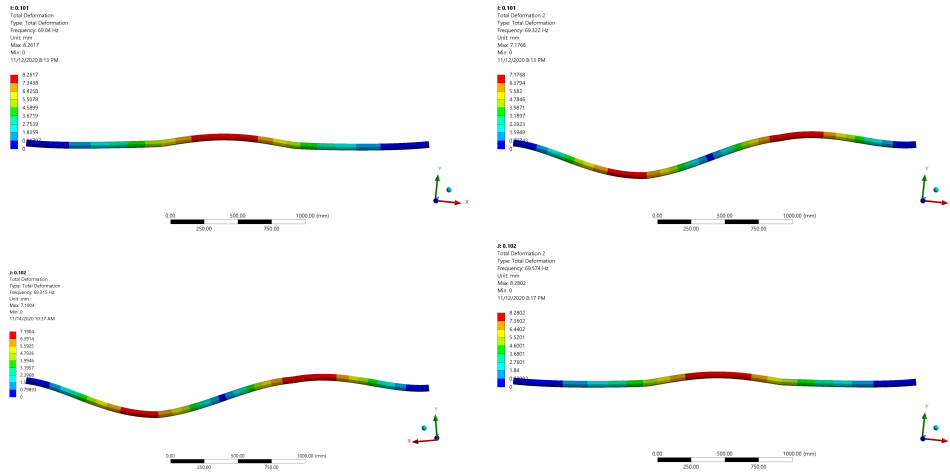| P	Source	ω_1 [Hz]	ω_2 [Hz]
0.101	This paper	437.618	437.925
0.101	FME	433.791	435.563
0.101	Reference [6]	437.614	437.869
0.102	This paper	437.889	441.001
0.102	FME	435.525	437.146
0.102	Reference [6]	437.834	440.997

FIGURE 12. Crossing phenomenon: a) – 1st mode, $p = 0.101$ $\omega = 433.791$ Hz; b) – 2nd mode, $p = 0.101$ $\omega = 435.563$ Hz; c) – 1st mode, $p = 0.102$ $\omega = 435.525$ Hz; d) – 2nd mode, $p = 0.102$ $\omega = 437.146$ Hz

Comparative results, obtained in the vicinity of the angle $p = p^*$, show that the referent values of circular natural frequencies obtained using the presented analytical form of the frequency equation are superior to those obtained using FEM analysis.

Figure 12 presents the results of the FEM computations in Ansys for the first two mode shapes. It can be noticed that the changes in a thousandth part of a radian cause switching among mode shapes, which is typical for the crossing phenomenon.

6. Conclusions

The paper presents the original numerical procedure for solving the system of partial differential equations of coupled axial and bending vibrations of Euler–Bernoulli beams within the framework of planar serial frame structures. The cross-section can be arbitrarily changed along the beam axis, whose dimensions must be within the validity of the Euler–Bernoulli theory. This also applies to the material density and Young's modulus of elasticity, which is the case in axially functionally graded materials. The procedure can be supported by any standard mathematical program package that contains programs for solving Cauchy's problem (MATHEMATICA®, MATLAB®,...) and can be applied easily to a larger number of beams.

Verification of numerical results obtained by this procedure can always be performed by FEM analysis, for natural frequencies and mode shapes. However, the presented application of the SNMIP method is superior to FEM analysis when qualitative and quantifying influences of some parameters on the natural frequencies themselves and mode shapes are analyzed, because it allows us to easily obtain the function $F(\omega, p) = 0$. This fact particularly refers to investigating the veering and crossing phenomena.

The contribution of this work is also in deriving the orthogonality conditions and determining the closed-form solutions in the arbitrary case of initial conditions. Standard packages for FEM analysis do not have such a feature and cannot be applied when it is necessary to determine the structure response in the time domain.

The procedure can also be generalized without any major problems to some more complex boundary conditions between beams, or at the structure ends such as embedded rigid bodies of finite dimensions or some elastic elements. Also, the proposed methodology can be applied to the buckling problem of planar serial frame structures, with minor modifications. Namely, the differential equations (2.1) should be replaced with the equations that are valid for the buckling problem accompanied with the appropriate analysis. This will be the topic of our next paper in this field.

References

1. H. P. Lin, J. Ro, *Vibration analysis of planar serial-frame structures*, J. Sound. Vib. **262** (2003), 1113–1131.
2. A. R. Ratazzi, D. V. Bambill, C. A. Rossit, *Free vibrations of beam system structures with elastic boundary conditions and an internal elastic hinge*, Ch. J. Eng. **2013** (2013), 1–10.
3. J. Ding, W. Zhuang, P. Wang, *Study on the seismic response of a portal frame structure based on the transfer matrix method of multibody system*, Adv. Mech. Eng. **2014** (2014), 1–10.
4. H. P. Lin, S. C. Chang, C. Chu, *Modal characteristics of planar multi-story frame structures*, J. Mech. **32** (2016), 501–514.
5. A. Obradović, S. Šalinić, D. R. Trifković, N. Zorić, Z Stokić, *Free vibration of structures composed of rigid bodies and elastic beam segments*, J. Sound. Vib. **347** (2015), 126–38.
6. A. Tomović, S. Šalinić, A. Obradović, A. Grbović, M. Milovančević, *Closed-form solution for the free axial-bending vibration problem of structures composed of rigid bodies and elastic beam segments*, Appl. Math. Model. **77** (2020), 1148–1167.
7. S. Tornincasa, E. Bonisoli, P. Kerfriden, M. Brino, *Investigation of crossing and veering phenomena in an isogeometric analysis framework*, Proceedings of the 32nd IMAC, 2014, 361–376.
8. C. Pierre, *Mode localization and eigenvalue loci veering phenomena in disordered structures*, J. Sound. Vib. **126**(3) (1988), 485–502.
9. X. L. Liu, *Behavior of derivatives of eigenvalues and eigenvectors in curve veering and mode localization and their relation to close eigenvalues*, J. Sound. Vib. **256**(3) (2002), 551–564.
10. E. Bonisoli, C. Delprete, M. Esposito, J. E. Mottershead, *Structural dynamics with coincident eigenvalues: Modelling and testing*, Conf. Proc. Soc. Exp. Mech. Ser. **6** (2011), 325–337.
11. S. Šalinić, A. Obradović, A. Tomović, *Free vibration analysis of axially functionally graded tapered, stepped, and continuously segmented rods and beams*, Compos. B. Eng. **150** (2018), 135–143.
12. A. Tomović, *Coupled Transverse and Longitudinal Vibrations of Euler–Bernoulli and Timoshenko Beams of Functionally Graded Materials*. Doctoral Dissertation, University of Belgrade, Faculty of Mechanical Engineering, Belgrade, 2019. (in Serbian)
13. J. Ṙ. Banerjee, A. Ananthapuvirajah, *An exact dynamic stiffness matrix for a beam incorporating Rayleigh–Love and Timoshenko theories*, Int. J. Mech. Sci. **150** (2019), 337–347.
14. J. R. Banerjee, A. Ananthapuvirajah, *Coupled axial-bending dynamic stiffness matrix for beam elements*, Comput. Struct. **215** (2019), 1–9.
15. S. Caddemi, I. Caliò, *The exact explicit dynamic stiffness matrix of multi-cracked Euler–Bernoulli beam and applications to damaged frame structures*, J. Sound Vib. **332**(12) (2013), 3049–3063.
16. S. S. Rao, *Vibration of Continuous Systems*, John Wiley & Sons, New Jersey, 2007.
17. L. Meirovitch, *Fundamentals of Vibrations*, McGraw-Hill, NewYork, 2001.
18. V. Vujičić, *Theory of Vibrations*, Naučna knjiga, Beograd, 1977. (in Serbian)
19. V. L. Biderman, *Theory of Mechanical Vibration*, Vysshaya Shkola, Moscow, 1980. (in Russian)
20. Wolfram Research, Inc., *Mathematica*, Version 12.0

СЛОБОДНЕ НЕПРИГУШЕНЕ ОСЦИЛАЦИЈЕ РАВАНСКИХ ОКВИРНИХ НОСАЧА ЗА СЛУЧАЈ АКСИЈАЛНО ФУНКЦИОНАЛНО ГРАДИЈЕНТНИХ МАТЕРИЈАЛА

Резиме. У раду се разматра модална анализа и налажење решења у затвореном облику слободних непригушених осцилација раванских оквирних носача, који се састоје од Ојлер-Бернулијевих греда променљивог попречног пресека за случај аксијално функционално градијентних материјала. Свака од тих греда врши спрегуте уздужне и попречне осцилације, где спрега настаје услед контурних услова на њиховим спојевима. Нумеричко решавање система парцијалних диференцијалних једначина, након раздвајања променљивих, своди се на двотачкасти гранични проблем система обичних линеарних диференцијалних једначина са променљивим коефицијентима и линеарним контурним условима. У том случају могућ је пренос граничних услова и свођење проблема на Кошијев проблем почетних услова. Такође је могуће анализирати и утицај појединих параметара на динамичко понашање. Метод се може применити за различите случајеве контурних услова на крајевима структуре, што је илустровано на одговарајућем нумеричком примеру.

Faculty of Mechanical Engineering
University of Belgrade
Belgrade
Serbia

Faculty of Mechanical and Civil Engineering in Kraljevo
University of Kragujevac
Kraljevo
Serbia

Faculty of Mechanical Engineering
University of Belgrade
Belgrade
Serbia